Comparison of batch and continuous multi-column protein A capture processes by optimal design

Daniel Baur[1], Monica Angarita[1], Thomas Müller-Späth[1,2], Fabian Steinebach[1] and Massimo Morbidelli[1]

[1] Department of Chemistry and Applied Biosciences, ETH Zurich, Zurich, Switzerland
[2] ChromaCon AG, Zurich, Switzerland

Multi-column capture processes show several advantages compared to batch capture. It is how-ever not evident how many columns one should use exactly. To investigate this issue, twin-column CaptureSMB, 3- and 4-column periodic counter-current chromatography (PCC) and single column batch capture are numerically optimized and compared in terms of process performance for cap-turing a monoclonal antibody using protein A chromatography. Optimization is carried out with respect to productivity and capacity utilization (amount of product loaded per cycle compared to the maximum amount possible), while keeping yield and purity constant. For a wide range of process parameters, all three multi-column processes show similar maximum capacity utilization and performed significantly better than batch. When maximizing productivity, the CaptureSMB process shows optimal performance, except at high feed titers, where batch chromatography can reach higher productivity values than the multi-column processes due to the complete decoupling of the loading and elution steps, albeit at a large cost in terms of capacity utilization. In terms of trade-off, i.e. how much the capacity utilization decreases with increasing productivity, Cap-tureSMB is optimal for low and high feed titers, whereas the 3-column process is optimal in an intermediate region. Using these findings, the most suitable process can be chosen for different production scenarios.

Keywords: Model based optimization · Monoclonal antibody · Periodic counter-current chromatography · Protein A affinity chromatography · Sequential capture

1 Introduction

Due to their fast growing market share and high value, monoclonal antibodies (mAbs) are one of the most important classes of biopharmaceuticals today [1]. Rapid progress in cell line development, resulting in greatly increased fermentation productivity and titers [2, 3] has increased the output of existing bioreactors and prompted the use of smaller fermenters and flexible manufacturing for new products. These developments require high-productivity, flexible downstream processes. Continuous upstream has become an attractive option in many cases, triggering the use of continuous downstream processes. In order to fulfill these requirements, novel downstream processes have been developed in the recent years, specifically in the field of chromatography, which is still the main process step in downstream purification [4, 5]. While the use of SMB technology has a long history in downstream processing [6–8], its operating principles (binary separation, many columns) make it generally a sub-optimal choice for affinity capture or polishing steps, where usually a ternary separation must be carried out. The new continuous chromatographic processes operate with two or more identical columns, enabling also counter-current principles. For polishing steps, multi-column counter-current solvent gradient purification (MCSGP) [9–12], has been successfully used and displayed supe-

Received 06 Aug 2015
Received 23 Dec 2015
Accepted 09 Mar 2016
Available online 15 Mar 2016

Correspondence: Prof. Massimo Morbidelli, Institute for Chemical and Bioengineering, Department of Chemistry and Applied Biosciences, ETH Zurich, Vladimir-Prelog-Weg 1, CH-8093 Zurich, Switzerland
E-Mail: massimo.morbidelli@chem.ethz.ch

Abbreviations: mAb, Monoclonal antibody; **PCC**, Periodic counter-current chromatography; **SMB**, Simulated moving bed; **SMCC**, Sequential multi-column chromatography; **CIP**, Cleaning in place

rior performance compared to batch chromatography. It has been shown that for protein A capture of mAbs, it can be advantageous to use multi-column setups, rather than batch chromatography, such as the twin-column CaptureSMB process (which is semi-continuous when an interconnected wash is applied) [13] or continuous processes with more columns, such as sequential multi-column chromatography (SMCC) processes [14, 15], or periodic counter-current (PCC) processes with interconnected wash, which are typically run with three or four columns [16, 17], or the BioSMB process, which uses up to 12 columns [18]. In general, counter-current chromatography offers several advantages, mainly increased productivity, better resin utilization and smaller specific buffer consumption, but these come at the price of higher hardware complexity and increased investment cost [19].

Common among these multi-column setups is that the product breakthrough of one column is directed into another column to adsorb, allowing the use of higher loading flow rates and loading times without compromising yield by product breaking through. This leads to higher productivity and higher loadings of the resin. Resin capacity utilization is proportional to product pool concentration and inversely proportional to buffer consumption and resin costs [13].

For many years, modeling has been a valuable tool for understanding and optimizing these multi-column processes, precisely because of the high investment costs and typically the high value of the products involved [20, 21]. A novel modeling approach for the diffusive behavior of the monoclonal antibodies inside the affinity resin particles, based on a shrinking core model, is applied here. It has been shown previously that fitting batch breakthrough experiments is sufficient for predicting the performance of the CaptureSMB process [22]. With the column model available, the capture process can be laid out in order to maximize two objectives: Productivity, that is mAb produced per column volume (CV) and time, and capacity utilization, that is how much mAb is loaded onto the columns compared to the maximum theoretically possible amount. It is possible to identify operating points biased towards one or the other objective, depending on manufacturing needs or cost targets. In this work we show that the trade-off is present for all investigated processes with one to four columns. Comparing the processes under these important aspects might shed some light on their advantages, disadvantages and usefulness for capture applications.

2 Process descriptions

As an example capture problem in this work, the purification of an IgG_1 monoclonal antibody (mAb) from clarified cell culture harvest is considered. The processes examined here are: single-column batch capture, twin-column CaptureSMB [13], and periodic counter-current (PCC) processes with interconnected wash step with three (3C-PCC) and four (4C-PCC) columns [16, 23] (Fig. 1). Note that the recovery and regeneration phase can be optimized separately and is independent of the process type. The total column volumes of buffers used in the different steps of the recovery and regeneration phase are assumed to be the same in all processes. Moreover it was assumed that the same recovery and regeneration protocol was used in every cycle. Therefore, it is not part of the optimization considered in this work. All flow rates of the recovery and regeneration phase that are not associated with loading, namely interconnected wash, wash, elution and equilibration, are assumed to be run at a constant flow rate Q_{RR} of 1.5 mL min^{-1} (corresponding to a linear velocity of 450 cm h^{-1}). The cleaning in place (CIP) step uses a constant contact time, i.e. its duration is independent on column size. The described processes have in common that steps with sequential loading of two columns and steps with single column loading alternate, each pair of these steps is referred to as "switch" in the following. However, in 3C- and 4C-PCC processes, the interconnected loading step and the recovery and regeneration procedure run simultaneously while in CaptureSMB they run sequentially.

2.1 CaptureSMB

The CaptureSMB process uses two columns, as shown in the process schematic in Fig. 1 (panel A, top). A detailed description is available in [13]. During the interconnected phase, which has the duration t_{IC}, the columns are loaded in series, with the flow rate Q_{IC}. After the columns have been loaded in series, a first interconnected wash step is performed at the end of the interconnected phase to flush any protein still present in the liquid phase into the second column. After this wash step, the first column is fully loaded and the columns are disconnected. While the first column enters the recovery and regeneration procedure the second column continues to be loaded. This step is denoted as the "batch" phase, with a duration of t_B, and a loading flow rate of Q_B for the second column.

Of the four design variables, three can be used to design the process (t_{IC}, Q_{IC} and Q_B), with the constraint that no breakthrough should occur, ensuring high yield in all operating points. Since the first column undergoes recovery and regeneration during the batch phase, the duration of this step, t_B, is fixed by the recovery and regeneration protocol, which ensures constant purity and product quality.

2.2 3-column PCC (3C-PCC)

The 3-column PCC process uses three identical columns. A process schematic, adapted from [24], can be found in Fig. 1 (middle panel B). A different 3C-PCC process has

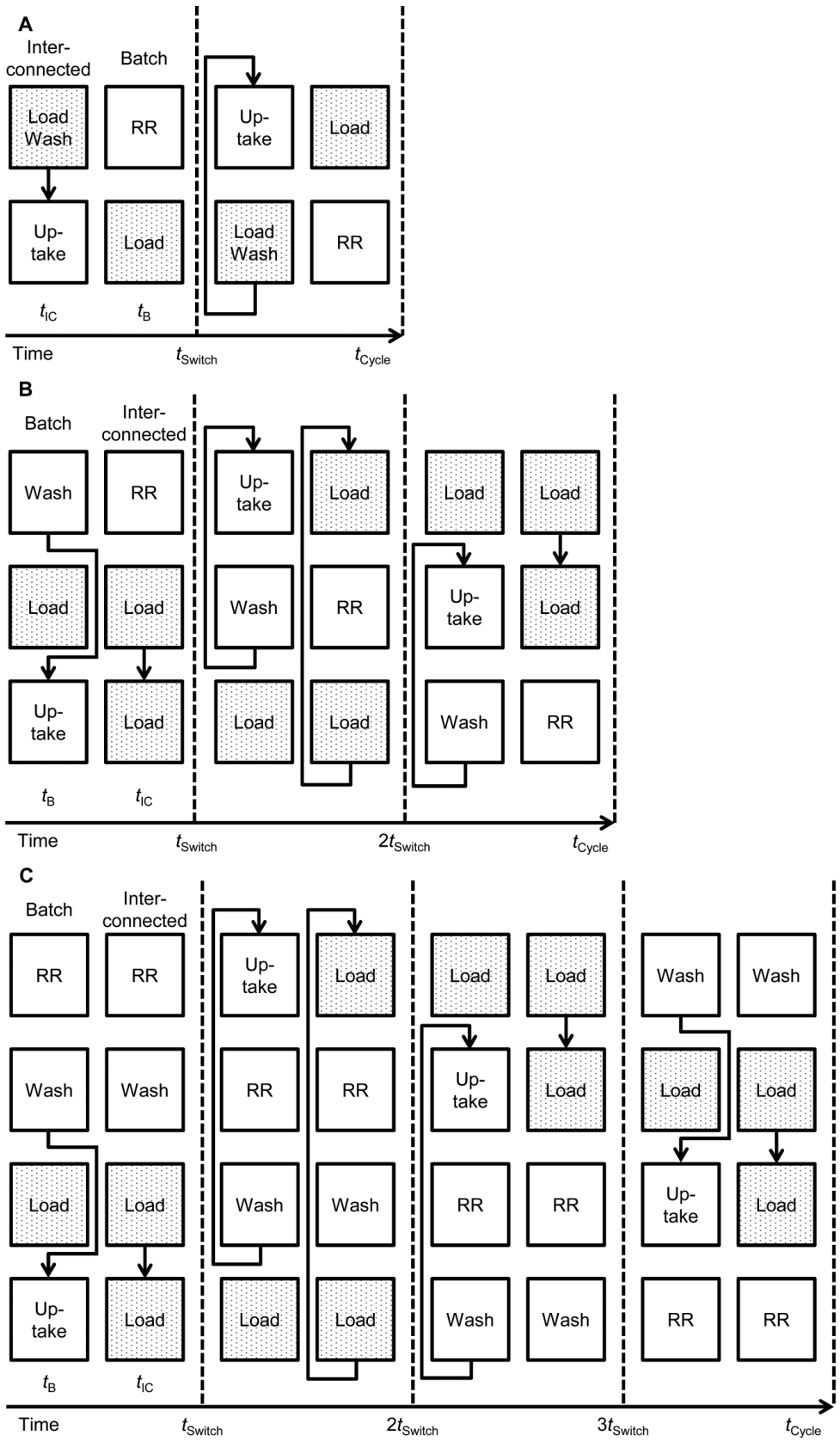

Figure 1. Flow chart of the multi-column processes. (**A**) CaptureSMB; (**B**) 3-column PCC; (**C**) 4-column PCC. For each process, an entire cycle is shown.

been published by the same group in [23], however in this work we refer to the newer process. In the 3-column PCC process, the first part of a switch consists of an interconnected wash step where the first, fully loaded column is washed and the wash is recycled into the third column, while the second column is loaded in a disconnected mode. Since the feed is applied to a disconnected column, this phase is denoted as the batch phase, with the duration t_B and the feed flow rate Q_B.

When the interconnected wash step is finished, the first and the third column are disconnected and the first column continues in the recovery and regeneration procedure, with further wash steps, the elution, the CIP and the equilibration step. In the meantime, the two other columns are loaded in an interconnected manner using a flow rate Q_{IC}; therefore this part of the switch is called the interconnected phase, which lasts for the time t_{IC}. After the interconnected phase is complete, all columns are moved one position upstream relative to the liquid phase flow, which denotes the beginning of a new switch. When three switches have passed and the columns are back in the initial configuration, one cycle has passed.

The duration of the interconnected wash dictates the duration of the batch step. The duration of the recovery and regeneration procedure, which happens during the interconnected phase, puts a lower bound on the duration of this step, since it is permitted to load for a longer time than it takes to wash, elute, clean and equilibrate one column. It is therefore permitted that the first column is inactive for certain periods of time following recovery and regeneration. The 3-column PCC process has three degrees of freedom, namely the two loading flow rates Q_B and Q_{IC} and the interconnected loading time t_{IC}.

2.3 4-column PCC (4C-PCC)

The 4-column PCC process uses four identical columns that are loaded and eluted sequentially [16]. A process schematic can be found in Fig. 1 (bottom panel C). In the setup investigated in this work, there are two different steps, during which different columns are interconnected.

In the first part of the switch, the column in the first position, which has been washed in the previous switch, is eluted. Meanwhile, the second column undergoes the first part of the wash step, during which product from the liquid phase of the first column is directed to the cleaned and regenerated column in the last position. During this time, the column in the third position is disconnected and loaded with feed with a flow rate of Q_B. Since the loading happens in a single column batch manner in this part of the switch, it is denoted as the batch phase, which has the duration t_B.

When the interconnected part of the wash step is completed, the second column is disconnected and the recovery and regeneration continues, with further washing. The elution of product from the first column finishes during this phase, and cleaning in place (CIP) and regeneration follow. Meanwhile, the other two columns are interconnected and further feed is applied to the third column, with a different flow rate Q_{IC}. After this, one switch has passed and the columns are moved one position upstream, i.e. counter-currently relative to the direction of the liquid phase flow. Because the feed is applied to two interconnected columns in this part of the switch, it is denoted as the interconnected phase with a duration of t_{IC}.

Since the interconnected wash step is fixed, the duration of the batch step, t_B, is fixed. However, it is again permitted to load for a longer time than it takes to clean and equilibrate a column and the first column is permitted to be inactive after regeneration, so there is a lower bound on the interconnected time t_{IC}. Therefore, the 4-column PCC process has three degrees of freedom, namely the two loading flow rates Q_B and Q_{IC} and the interconnected time t_{IC}.

3 Materials and methods

The cell culture supernatant used in the experimental parts of this study was produced at ETH Zurich by continuous fermentation and contained a monoclonal IgG_1-type antibody in concentrations between 0.20 and 0.75 mg mL^{-1}. For the breakthrough experiments at higher concentrations, clarified cell culture supernatant with a concentration of 0.3 mg mL^{-1} was spiked with elution product of previous capture runs to obtain feed concentrations of 1.5 mg mL^{-1} and 2.5 mg mL^{-1}. As stationary phase, MabSelect SuRe (GE Healthcare Life Sciences), in pre-packed columns of dimensions 0.5 × 5 cm (Atoll, Weingarten, Germany) was used for all experiments. Two such columns were joined in series to form columns with bed heights of 10 cm. The preparative conditions and analytical method (analytical protein A chromatography) were the same as reported in [22], with two differences in the preparative part: The duration of the CIP step was varied as a process variable, and recovery and regeneration was always performed at maximum flow rate, therefore $Q_{RR} = Q_{max}$.

3.1 Process model

Since adsorption of mAbs on protein A ligands is very fast compared to diffusion through the resin particles, the radial profile of adsorbed protein in the particles shows a very steep front, as has been shown in theory and also experimentally by confocal x-ray spectroscopy [25–29]. This property is used as a basis for a model that avoids completely the radial discretization of the resin particles. Shrinking core models have been proposed previously for catalyzed chemical reactions in porous particles [30], and the analogy between a fast chemical reaction and an

adsorption process justifies its use in chromatography. Therefore, the same approach is used to describe the moving front of adsorbed protein.

3.2 Shrinking core adsorption model

According to the shrinking core model, the protein has to diffuse through a stagnant film between the bulk phase and the solid phase particle, and a layer of antibody-saturated protein A sites of thickness $r_p - R$, where r_p is the resin particle radius and R is the radial position of the antibody front progressing through the particle, before adsorbing on a free protein A adsorption site. This process is visualized in Fig. 2. The total mass transfer coefficient is therefore given as a combination of these two contributions:

$$k_{tot} = \left(\frac{1}{k_F} + \frac{1}{k_S} \right)^{-1} \tag{1}$$

where k_F is the film mass transfer coefficient and k_S is the pore mass transfer coefficient. By combining the fact that the molar flow rate of the protein through the saturated layer is constant, and by using a linear driving force assumption, the following expression can be used to calculate the pore mass transfer coefficient [31]:

$$k_S = D \frac{(1-\alpha)^{1/3}}{1-(1-\alpha)^{1/3}} \tag{2}$$

where $D = \varepsilon_p D_E / r_p$ is a fitting parameter that is related to the pore diffusion coefficient for diffusion through saturated pores D_E and α is the fraction of total adsorption sites occupied, i.e.

$$\alpha = \frac{q_1}{q^*_{Feed}} = \frac{q_1}{q_{sat}} \frac{1/K_D + c_{Feed}}{c_{Feed}} \tag{3}$$

where q_1 is the solid phase concentration on the first adsorption site (Eq. 6), q^*_{Feed} is the equilibrium solid phase concentration of protein at feed concentration, q_{sat} is the saturation capacity of the resin, c_{Feed} is the protein concentration in the feed and K_D is the equilibrium constant of the adsorption process.

The film mass transfer coefficient k_F on the other hand can be estimated from a classical semi-empirical correlation [4]:

$$k_F = \frac{D_0}{2r_p} \cdot \frac{1.09}{\varepsilon_B} \left(\frac{2r_p u}{D_0} \right) \tag{4}$$

where D_0 is the protein diffusivity in free solution, ε_B is the porosity of the packed bed and $u = Q/A_{Col}$ is the superficial velocity, where Q is the volumetric flow rate, and A_{Col} is the column cross sectional area.

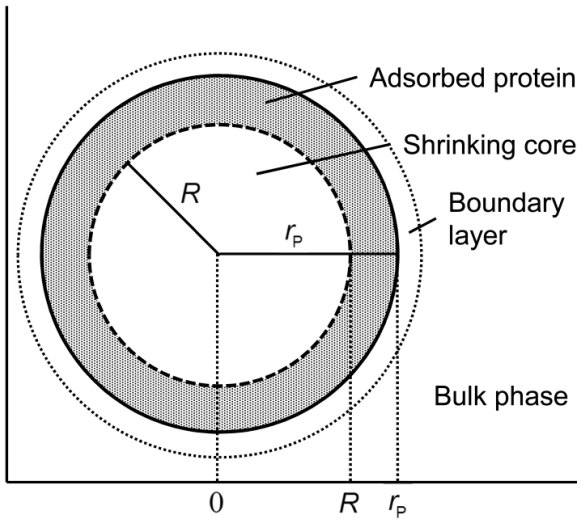

Figure 2. Visualization of the moving front inside a resin particle according to the shrinking core model.

The intra-particle liquid phase is therefore described by the equilibrium with the bulk liquid phase and the adsorption terms:

$$\frac{\partial c_P}{\partial t} = \frac{3k_{tot}}{r_p}(c - c_P) - \phi_P \cdot \left(\frac{\partial q_1}{\partial t} + \frac{\partial q_2}{\partial t} \right) \tag{5}$$

where c_P is the intra-particle liquid phase concentration, c is the bulk liquid phase concentration, $\phi_P = (1 - \varepsilon_P)/\varepsilon_P$ is the particle phase ratio, where ε_P is the particle porosity, and q_i are the adsorbed phase concentrations for each adsorption site. The particle porosity, and therefore the intra-particle liquid phase volume, is assumed to be independent of adsorption and therefore constant.

For immobilized recombinant protein A ligands two to three adsorption sites are actually available per ligand [4], and since the adsorption rate constant decreases with increasing number of mAbs bound to a ligand due to steric hindrance, only the first two adsorption possibilities are taken into account here. This leads to the following expressions for the change in adsorbed phase concentrations [31]:

$$\begin{aligned} \frac{\partial q_1}{\partial t} &= k_{A,1} \left[c_P (q_{sat} - q_1) - \frac{q_1}{K_D} \right] \\ \frac{\partial q_2}{\partial t} &= k_{A,2} \left[c_P (q_1 - q_2) - \frac{q_2}{K_D} \right] \end{aligned} \tag{6}$$

where $k_{A,i}$ are the adsorption rate constants for each site. Note that in the formula for the second adsorption site, the current concentration of the first site appears in place of the saturation capacity. This reflects the fact that the second site is a hindered site, which can only be occupied when a mAb is already adsorbed on the first site.

3.3 Column model

As in the standard lumped kinetic model, the equations above describing the adsorption process are combined with the transport equations for the liquid phase [20]:

$$\frac{\partial c}{\partial t} = -v\frac{\partial c}{\partial x} + D_L\frac{\partial^2 c}{\partial x^2} - \frac{3k_M}{r_P}(c - c_P)$$
$$t \in [0, t_{Switch}], \quad x \in [0, L_{Col}] \tag{7}$$

where t denotes the time, $v = u/\varepsilon_B$ is the interstitial velocity, x is the coordinate along the longitudinal axis of the column, D_L is the apparent axial dispersion coefficient, and L_{Col} is the bed height of one column.

These partial differential equations are subject to the following boundary conditions and initial conditions:

$$\begin{aligned} c(t=0,x) &= c_0(x) \\ c_P(t=0,x) &= c_{P,0}(x) \\ q_i(t=0,x) &= q_{i,0}(x) \\ c(t,x=0) &= c_{In}(t) + \frac{D_L}{v}\left.\frac{\partial c}{\partial x}\right|_{x=0} \\ \left.\frac{\partial c}{\partial x}\right|_{x=L_{Col}} & \end{aligned} \tag{8}$$

The apparent axial dispersion coefficient was estimated as described in [22], and the same solution procedure was used to solve the system of partial differential equations.

3.4 Process performance measures and optimization problem

Apart from impurity clearance, the three most important performance measures in preparative affinity chromatography are yield, productivity and capacity utilization. Since the main factors influencing product purity are the type of stationary phase and the recovery and regeneration protocol, it is not modelled and considered constant and in specification for all investigated processes. Yield and productivity by contrast are strongly influenced by the operating parameters, namely the flow rates and durations of the different process steps, and they are properly calculated in the model. In capture processes, columns are typically not fully loaded since this would compromise yield. In batch capture of monoclonal antibodies for example, 90% of the volume corresponding to 1% breakthrough [16] is loaded to ensure maximum and constant yield. Since this does not directly translate to multi-column processes and different implementations of a safety factor will make a fair comparison difficult, the constraint applied for all processes in this work is that the breakthrough value of a disconnected column must not exceed 1%. This assures a high yield value for all processes considered.

Flow rate constraints were implemented based on product information provided by the manufacturer. For MabSelect SuRe a maximum linear velocity of 500 cm h^{-1} is reported, resulting in a maximum flow rate of Q_{max} = 1.67 mL min^{-1} (GE Healthcare, Data file 11-0011-65 AC, retrieved online 07/2014).

It is important to highlight that the processes described were not optimized under a feed continuity constraint as described in [24] for full integration with continuous upstream manufacturing without an intermediate balancing container. Instead, a setup as described in [23] was assumed, with a balancing container ("surge bag") at the interface of upstream and downstream processing. This setup requires only the average inflow and outflow of the container to be equal, allowing flexible feed flow rates on the side of the downstream capture, i.e. different feed flow rates in the interconnected and batch phases of multicolumn capture, allowing better process performance. Moreover this setup appears advantageous from a risk perspective. It also covers the state-of-the-art mAb fed-batch fermentation, where the entire harvest becomes available at a certain point in time. Due to the risk of product degradation, this scenario requires the harvest to be processed within a certain time period, typically around 24 h, however this capture mode does not require the feed flow rate to be constant.

The first optimization target is productivity, which is defined as the amount of product produced per resin volume and unit time and can be written as follows for all processes:

$$P = Y \cdot \frac{c_{Feed}(t_{IC}Q_{IC} + t_B Q_B)}{n_{Col}V_{Col}(t_{IC} + t_B)} \tag{9}$$

where Y is the process yield, c_{Feed} is the mAb concentration in the feed, n_{Col} is the number of columns the process uses, and $V_{Col} = L_{Col} \cdot A_{Col}$ is the volume of one column. Note that for batch chromatography, there is no interconnected phase, and the recovery and regeneration time has to be added to the switch time in the denominator.

The second optimization target is the capacity utilization CU, which is defined as the actual load per cycle divided by the maximum possible load. Therefore, the higher the capacity utilization, the more antibody can be produced per volume of resin before the resin needs to be replaced, since fewer load and elute cycles are needed to process a given amount of antibody. Thus, higher capacity utilization leads to lower resin costs. The capacity utilization can be calculated as follows:

$$CU = Y \cdot \frac{c_{Feed}(t_{IC}Q_{IC} + t_B Q_B)}{(1-\varepsilon_B)V_{Col}q_{max}} \tag{10}$$

where q_{max} is the maximum possible amount that could theoretically be loaded per column volume at a given feed concentration, which can be calculated as follows:

$$q_{max} = \frac{c_{Feed}}{(1/K_D + c_{Feed})} q_{sat} \quad (11)$$

Summarizing the constraints and objectives discussed above, the following optimization problem can be formulated:

$$\begin{array}{lll} \underset{x}{\text{maximize}} & P(x), CU(x) & \\ \text{subject to} & c(z = L_{Col}) & \leq 0.01 c_{Feed} \\ & Q & \leq Q_{max} \\ & 0 & < x \\ & t_{RR} & \leq t_{IC} \end{array} \quad (12)$$

where x are the degrees of freedom of the capture process with $x = [t_B, Q_B]$ as the degrees of freedom for batch single column chromatography and $x = [Q_B, t_{IC}, Q_{IC}]$ as degrees of freedom for the multicolumn processes. Note that the first constraint $c(z = L_{Col}) \leq 0.01 c_{Feed}$ is, as mentioned above, effectively a yield constraint that applies only for columns that are being loaded and have no column connected to their outlet. This effectively assures that the first column in the loading zone is loaded to a very high breakthrough value (typically above 60%) as well. The last constraint $t_{RR} \leq t_{IC}$ only applies to the 3- and 4-column PCC processes. For numerical optimization, a multi-objective genetic algorithm, i.e. a modified version of the third iteration of the generalized differential evolution algorithm (GDE3) was used [31].

4 Results and discussion

4.1 Model fitting of batch protein A breakthrough curves

From the breakthrough experiments described in the materials and methods section the parameters D, $k_{A,1,2}$, K_D, and q_{sat}, used in Eq. (2), (3) and (6) can be estimated. This is done by minimizing the sum of square errors using the GDE3 algorithm. 13 breakthrough curves at three different linear velocities between 150 and 450 cm h^{-1} (resulting in flow rates between 0.5 and 1.5 mL min^{-1}), and five different feed concentrations between 0.2 and 2.5 mg mL^{-1} were used to fit the model parameters. The data set includes columns with bed heights of 5 and 10 cm. A full list of all the parameters and their value is reported in Supporting information, Table S1. The intra-particle diffusion coefficient k_S and the film mass transfer coefficient k_F obviously depend on the solid phase and feed concentrations, and the current flow rate, respectively. The values of the intra-particle diffusion coefficient k_S were typically in the range of 0.001 cm min^{-1}, while the film mass transfer coefficient k_F was typically in the range of 10 cm min^{-1}. Therefore, as expected in protein chromatography, intra-particle diffusion was the rate limiting step. Several breakthrough curves with fitted model results are displayed in Fig. 3. Clearly the model is applicable for simulating breakthrough curves at different flow rates and different feed compositions, and can accurately account for different column lengths. The root mean square error in each experiment was in the range of 1.20 to 3.98%, averaging at 2.49%. As expected in protein

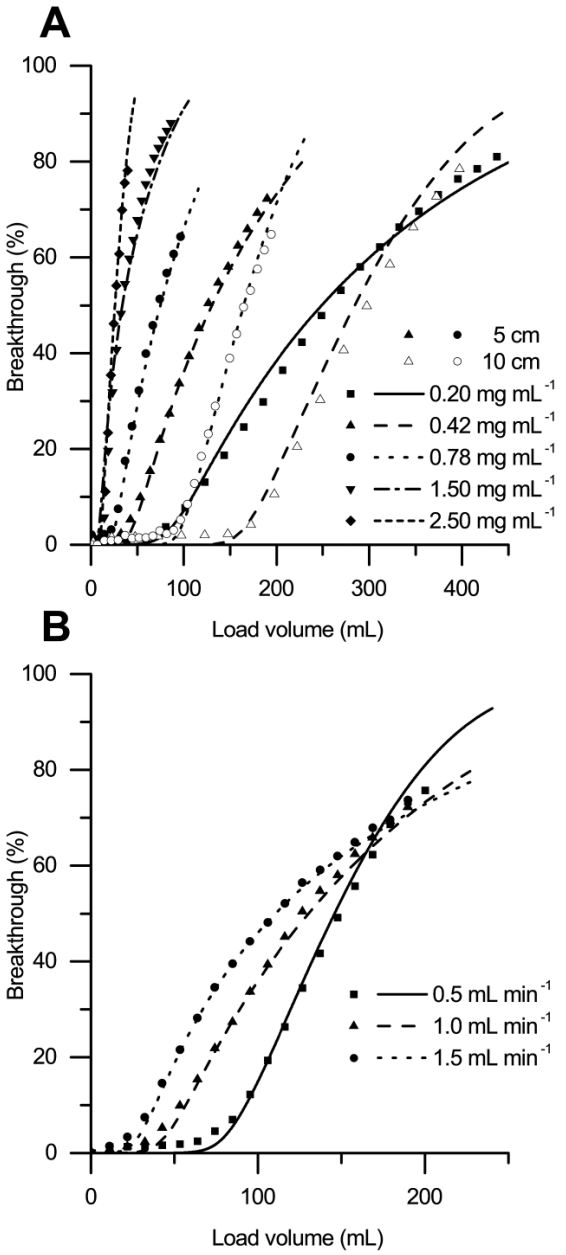

Figure 3. (**A**) Experimental breakthrough curves at different feed concentrations (symbols) compared with simulation data (lines). The feed flow rate was 1.0 mL min^{-1} (300 cm h^{-1}) for feed concentration below 1.0 mg mL^{-1}, 1.5 mL min^{-1} for the curve at 1.5 mg mL^{-1} and 0.75 mL min^{-1} (225 cm h^{-1}) for the curve at 2.5 mg mL^{-1}. (**B**) Experimental breakthrough curves at different feed flow rates (symbols) compared with simulation data (lines). The feed concentration was 0.42 mg mL^{-1}, the bed height was 5 cm and the column diameter was 0.5 cm in all cases.

A chromatography, the isotherm resulting from the fitted parameters is nearly rectangular. The isotherm is shown in Supporting information, Fig. S1.

4.2 Operational parameters considered for optimization

Along with the optimization, the influence of four different operational parameters on the optimal operating points of the capture processes was examined: The cleaning-in-place contact time, the number of column volumes used in the interconnected wash step, the bed height of a single column and the feed concentration. An overview of the cases examined is reported in Supporting information (Table S2). In a first scenario, the processes were optimized for cleaning (CIP) durations of 15, 30 and 60 min. In a second scenario the optimization was done for washing in series (interconnected) for 0, 3 and 6 column volumes, respectively. In a third scenario, the optimization was done for feed concentrations of 0.5, 1.5, 2.5, and 5.0 mg mL^{-1}. In the base case, for which a CIP time of 30 min, three column volumes interconnected wash and a feed concentration of 1.5 mg mL^{-1} was used, bed heights of 5 and 10 cm were considered, which results in loading zone bed heights of 5, 10 or 20 cm. Since columns with bed heights of less than 10 cm are generally not considered to be reproducibly packable at large scale, and minimal single column bed height appears to be optimal because this shortens the recovery and regeneration procedure, the investigation of the effect of changing the operational parameters was limited to 10 cm columns. Any scaling up can then be done by increasing the column diameter, which is not expected to have any impact on process performance unless radial flow distribution becomes an issue [4].

4.3 Base case optimization results in productivity/capacity utilization trade-off for all processes

Fig. 4 shows pareto-optimal operating points in the capacity utilization (CU) versus productivity plane for the base case, at fixed purity and yield values. The data confirm the expected trade-off of operating with high productivity but low capacity utilization or at high capacity utilization but low productivity. In terms of column bed heights, it is evident that with 5 cm bed height columns, a higher maximum productivity per column volume can be achieved than with 10 cm bed height columns for all processes. When comparing the different processes, the batch process is clearly inferior to the multi-column processes in terms of capacity utilization, but can achieve a similar maximum productivity value, although at the expense of a strong decrease in capacity utilization. Among the multi-column processes, the 4-column PCC process shows the worst performance, because more capacity utilization is lost when increasing the productivity. The CaptureSMB and 3-column PCC processes can achieve a similar maximum productivity, which is the highest maximum productivity for both bed heights. The multi-column processes all show a similar maximum capacity utilization close to 100%, independent of bed height. These operating points at high capacity utilization of course exhibit a corresponding decrease in productivity. In all cases considered, the pareto-fronts show the same behavior in terms of process constraints: Each and every pareto-optimal point has exactly 1% breakthrough (Eq. 12), which is obvious because as long as the breakthrough constraint is not active, one can simply load faster (increasing productivity) or more (increasing capacity utilization). The end points of the pareto-curves are marked by any other constraint becoming active: At maximum capacity utilization (and minimum productivity), the loading flow rates reach the lower bounds (set at 0.01 mL min^{-1} to avoid points where nothing is loaded at all), or the capacity utilization approaches 100%, where no further benefit can be gained by reducing the productivity. On the other hand, at maximum productivity (and minimum capacity utilization), either the maximum loading flow rate is reached, or, in the case of the multi-column processes, the minimum loading time due to the additional constraint that the regeneration of one column must be finished when a switch ends. Note that this minimum time is higher in the 3-column PCC process than in the 4-column PCC process, because the recovery and regeneration step is spread out over fewer columns, leading in some cases to abrupt stops in the pareto-curves. In the case of CaptureSMB, the fixed loading time in the

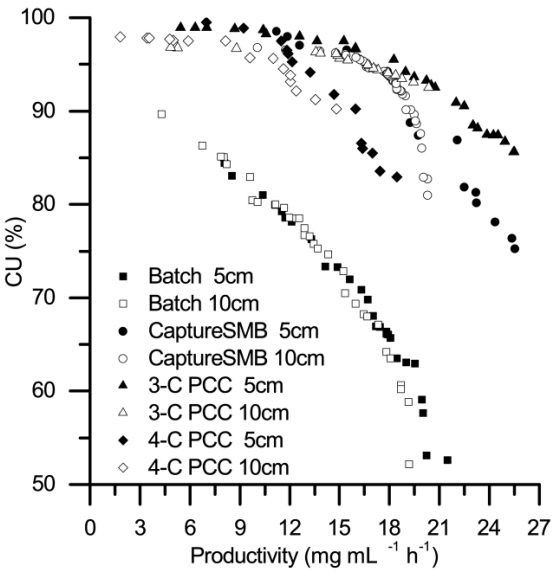

Figure 4. Pareto-optimal operating points (at fixed yield and purity) for the base case (t_{CIP} = 30 min, $Wash_{IC}$ = 3 CV, c_{Load} = 1.5 mg mL^{-1}). Filled symbols show results for 5 cm single column bed height, empty symbols show the results for 10 cm single column bed height.

batch phase is generally less of a concern because its impact can be diminished by reducing the batch loading flow rate.

In any case, if the minimum loading time is reached before the maximum loading flow rate is reached, any attempts to increase the productivity by increasing the loading flow rate or the loading time will simply result in yield loss, because the breakthrough constraint is already active, therefore negating any possible gains in productivity. This behavior is illustrated in Supporting information, Fig. S2. Different operating conditions may change the exact position of the steep drop relative to the optimum, but in no case this kind of yield loss is avoidable.

The model predicts an average increase in productivity of 39% when going from batch to CaptureSMB, which is in good agreement with the values reported in [13], where an average increase of 37.5% was found, albeit for a different IgG_1-type antibody. At high loading flow rates, which corresponds to operating points with high productivity, an average increase in capacity utilization of around 46% is predicted by the model, which corresponds well to the value of 42% that has been reported in [13].

4.4 Influence of CIP time

In the subsequent optimizations starting from the base case, the CIP time was varied. As can be seen in Fig. 5 (top, panel A), an increased CIP contact time leads to decreased maximum productivity in all processes. This is expected, as cleaning is "not productive" in the sense that no product is loaded or eluted during cleaning. It must be noted that the maximum capacity utilization is basically independent of CIP contact time. This is obvious in the case of batch chromatography, as the CIP step has no impact on the loading of the column. On the other hand, in the CaptureSMB process, a longer CIP time leads to a longer fixed loading time by increasing t_B, but this can be compensated by changing the batch loading flow rate and the interconnected time. In the PCC processes, a longer CIP time simply raises the lower bound on the interconnected loading time, so as long as this constraint is not active (which is the case at high capacity utilization, where the flow rates are low and the loading times are high), the CIP time has no impact on the loading. When comparing the different processes, the same trends as in the base case can be observed: the batch process is inferior in terms of capacity utilization, but can reach similar values of maximum productivity. Among the multi-column processes, again all processes can reach very high capacity utilization, and the CaptureSMB process can achieve slightly higher productivity than the 3-column PCC process, but at a larger cost in terms of capacity utilization. The 4-column PCC process again shows the worst performance among the multi-column processes.

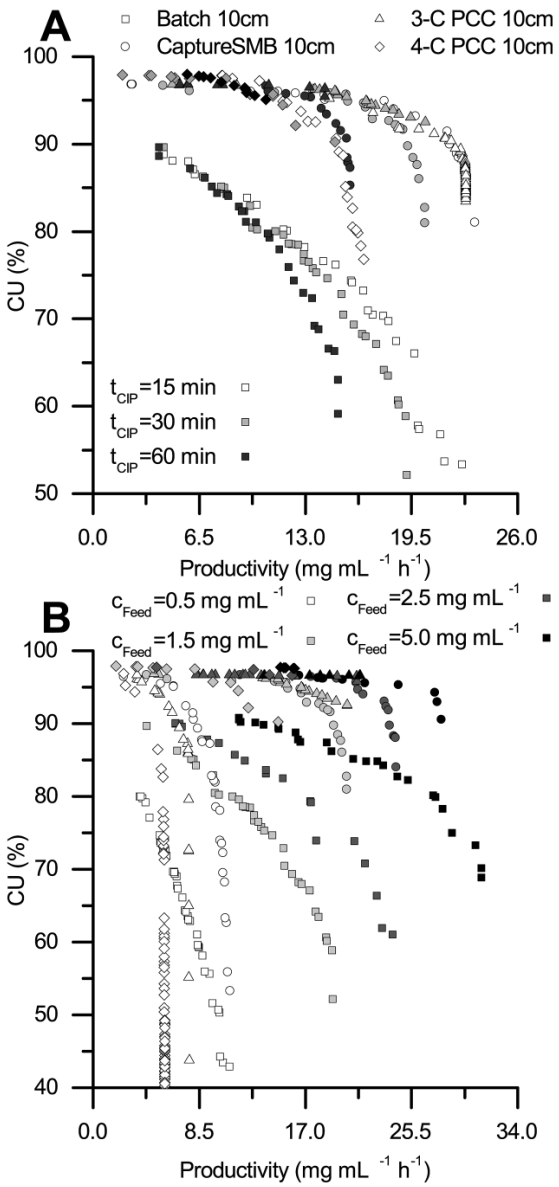

Figure 5. (**A**) Influence of changing t_{CIP} from 15 to 30 to 60 minutes. The other parameters correspond to the base case, i.e. three column volumes interconnected wash and 1.5 mg mL^{-1} feed concentration. (**B**) Effect of changing c_{Feed} between 0.5 and 5.0 mg mL^{-1}. The other parameters correspond to the base case.

4.5 Influence of feed concentration

Changing the feed concentration changes the behavior of the processes most significantly as can be seen in Fig. 5 (bottom, panel B). As expected, the maximum productivity increases with increased feed concentration for all processes. This improvement is mainly due to a decrease of the loading time, which decreases with increasing titer. With decreasing loading time, the time required for recovery and regeneration becomes dominant and

Table 1. Optimum process choice depending on feed titer and desired performance objective

Objective Feed titer	Productivity	Capacity utilization	Trade-off
Low (~0.5 mg mL^{-1})	CaptureSMB	CaptureSMB / 3- / 4-C PCC	CaptureSMB
Medium (1.5–2.5 mg mL^{-1})	CaptureSMB	CaptureSMB / 3- / 4-C PCC	3-column PCC
High (~5.0 mg mL^{-1})	Batch	CaptureSMB / 3- / 4-C PCC	CaptureSMB

the improvement in productivity levels off with increasing titer. On the other hand, the maximum achievable capacity utilization stays approximately constant. At lower feed concentrations, again batch is inferior to the multi-column processes in terms of capacity utilization. But in this region, the CaptureSMB process dominates the other processes. This is due to the fact that the maximum loading flow rate can be used without breakthrough being an issue, which causes the pareto-fronts to become vertical. In this case, additional columns convey no benefit. At higher feed concentrations, two changes can be observed: Firstly, the 3-column PCC process reaches its maximum productivity value before the CaptureSMB process exhibits any significant drop in capacity utilization, giving the CaptureSMB process a much better trade-off, in addition to its higher maximum productivity value. This is caused by the additional constraint on the loading time for the PCC processes ($t_{IC} \leq t_{RR}$) becoming active. Secondly, the batch process becomes more competitive in terms of maximum productivity, eventually outperforming all multi-column processes at 5.0 mg mL^{-1}. This can be explained by the fact that loading times become very short in this region, and the complete decoupling of loading and elution gives batch an advantage in this case. As in the other cases however, the batch process has a worse trade-off than the multi-column processes. It should be noted that the results for 5.0 mg mL^{-1} feed concentration are extrapolated data, as there were no experiments performed at this concentration. The main uncertainty introduced by this extrapolation concerns the assumption of a sharp shrinking core front inside the particles. This assumption becomes weaker because the mass transfer, which is proportional to the concentration gradient inside the particle, becomes faster. This should mainly impact the shape, but not the position of the breakthrough curves, which is only important to determine how much is recycled, but should have little impact on the process performances.

In conclusion, the optimal process choice depends on the feed titer and the desired objective (maximum productivity, maximum capacity utilization or best possible trade-off between the objectives). The best choice for each combination based on the optimization results is reported in Table 1. Of the processes examined, CaptureSMB offers the best trade-off, i.e. how much capacity utilization is lost when increasing the productivity, at low (<1.5 mg mL^{-1}) and high titers (>2.5 mg mL^{-1}). In the intermediate range, the 3-column PCC process exhibits the best trade-off. In terms of maximizing capacity utilization, it is clear that any of the multi-column processes is suitable for all feed titers, outperforming batch in every case. For achieving maximum productivity, CaptureSMB is optimal at low and medium titers (<2.5 mg mL^{-1}), while batch becomes optimal at high feed titers.

The two to four-column capture processes each contain an interconnected wash step that follows the sequential loading. The wash step is required to wash unbound material from the liquid volume of the first column into the second column for adsorption [16]. Moreover, due to change of the equilibrium conditions when flushing with wash buffer, product may desorb from the first column and needs to be captured in the second column requiring washing volumes of more than one column volume. The model predicts negligible impact on capacity utilization and productivity when changing the interconnected wash step for all multi-column processes. These results are shown graphically in Supporting information, Fig. S3.

5 Concluding remarks

Batch capture and three different continuous multi-column protein A mAb capture processes (2-column CaptureSMB and 3- and 4-column PCC) were numerically optimized and compared in different operating regimes with respect to capacity utilization and productivity, at constant yield and purity. The model used for this task was tuned on ad-hoc batch breakthrough experiments. This resulted in sets of pareto-optimal operating points, showing a trade-off between capacity utilization and productivity.

In the base case examined (three column volumes interconnected wash, 30 min CIP time, 1.5 mg mL^{-1} feed titer), the multi-column processes show a productivity increase from 5 to 19 mg mL^{-1} h^{-1} for the CaptureSMB, an increase from 5 to 20 mg mL^{-1} h^{-1} for the 3C-PCC, and an increase from 5 to 15 mg mL^{-1} h^{-1} for the 4C-PCC compared to the batch process at a fixed capacity utilization of 90%. On the other hand, at a fixed productivity of 14 mg mL^{-1} h^{-1}, an increase from 75% to 97% in capacity utilization is obtained for a fixed productivity when using CaptureSMB or 3C-PCC, and an increase from 75% to

90% is reached in the 4-column PCC process compared to batch capture.

The multi-column processes completely dominated the batch process in all cases (except when maximizing productivity at high titers), with the CaptureSMB showing best performance in terms of productivity and all three multi-column processes showing optimal and comparable performance in terms of capacity utilization. At both low and high feed concentrations, CaptureSMB showed the best trade-off situation, while the 3-column PCC process has the best trade-off in an intermediate region. When increasing the feed concentration to 5.0 mg mL^{-1}, an interesting change can be observed: In this case, the CaptureSMB process still has the best trade-off between capacity utilization and productivity, but the performance of the multi-column processes in terms of productivity drops off below the values achievable in the batch process, albeit at a considerable decrease in capacity utilization. This is due to the fact that there are additional constraints on the loading time in the multi-column processes, because sequential loading and recovery and regeneration are performed in parallel, which does not allow for fast enough loading to achieve higher productivity values. In all cases however, the improved capacity utilization provided by the multi-column processes translates into a proportional decrease in resin costs and buffer consumption, while product concentration increases proportionally.

Finally, it should be pointed out that the increased performance of the multicolumn processes comes at the cost of higher investments and more complex hardware. The hardware demand (pumps, valves, detectors, and piping) generally increases linearly with the number of columns. However, given that a step change in performance takes place when moving from a batch process to a two column process the increase in hardware investment can be justified since significant savings in operating expenditures and increased speed of processing is achieved. In conclusion, among the multicolumn processes for mAb capture the two column process is preferable as it combines minimum hardware investment and risk with maximum process performance and flexibility.

The authors declare no financial or commercial conflict of interest.

6 References

[1] Elvin, J. G., Couston, R. G., van der Walle, C. F., Therapeutic antibodies: Market considerations, disease targets and bioprocessing. *Int. J. Pharm.* 2013, *440*, 83–98.

[2] Walsh, G., Biopharmaceutical benchmarks 2014. *Nat. Biotechnol.* 2014, *32*, 992–1000.

[3] Hacker, D. L., De Jesus, M., Wurm, F. M., 25 years of recombinant proteins from reactor-grown cells — Where do we go from here? *Biotechnol. Adv.* 2009, *27*, 1023–1027.

[4] Carta, G., Jungbauer, A., *Protein Chromatography: Process Development And Scale-up*, John Wiley & Sons 2010.

[5] Low, D., O'Leary, R., Pujar, N. S., Future of antibody purification. *J. Chromatogr. B* 2007, *848*, 48–63.

[6] Andersson, J., Mattiasson, B., Simulated moving bed technology with a simplified approach for protein purification: Separation of lactoperoxidase and lactoferrin from whey protein concentrate. *J. Chromatogr. A* 2006, *1107*, 88–95.

[7] Gottschlich, N., Kasche, V., Purification of monoclonal antibodies by simulated moving-bed chromatography. *J. Chromatogr. A* 1997, *765*, 201–206.

[8] Mazzotti, M., Storti, G., Morbidelli, M., Optimal operation of simulated moving bed units for nonlinear chromatographic separations. *J. Chromatogr. A* 1997, *769*, 3–24.

[9] Aumann, L., Morbidelli, M., A continuous multicolumn countercurrent solvent gradient purification (MCSGP) process. *Biotechnol. Bioeng.* 2007, *98*, 1043–1055.

[10] Müller-Späth, T., Aumann, L., Melter, L., Ströhlein, G., Morbidelli, M., Chromatographic separation of three monoclonal antibody variants using multicolumn countercurrent solvent gradient purification (MCSGP). *Biotechnol. Bioeng.* 2008, *100*, 1166–1177.

[11] Aumann, L., Morbidelli, M., A semicontinuous 3-column countercurrent solvent gradient purification (MCSGP) process. *Biotechnol. Bioeng.* 2008, *99*, 728–733.

[12] Müller-Späth, T., Krättli, M., Aumann, L., Ströhlein, G., Morbidelli, M., Increasing the activity of monoclonal antibody therapeutics by continuous chromatography (MCSGP). *Biotechnol. Bioeng.* 2010, *107*, 652–662.

[13] Angarita, M., Müller-Späth, T., Baur, D., Lievrouw, R. et al., Twin-column CaptureSMB: A novel cyclic process for protein A affinity chromatography. *J. Chromatogr. A* 2015, *1389*, 85–95.

[14] Holzer, M., Osuna-Sanchez, H., David, L., Multicolumn chromatography. *Bioprocess Int.* 2008, *6*, 74–82.

[15] Ng, C. K. S., Rousset, F., Valery, E., Bracewell, D. G., Sorensen, E., Design of high productivity sequential multi-column chromatography for antibody capture. *Food Bioprod. Process.* 2014, *92*, 233–241.

[16] Mahajan, E., George, A., Wolk, B., Improving affinity chromatography resin efficiency using semi-continuous chromatography. *J. Chromatogr. A* 2012, *1227*, 154–162.

[17] Pollock, J., Bolton, G., Coffman, J., Ho, S. V. et al., Optimising the design and operation of semi-continuous affinity chromatography for clinical and commercial manufacture. *J. Chromatogr. A* 2013, *1284*, 17–27.

[18] Bisschops, M., Frick, L., Fulton, S., Ransohoff, T., Single-use, continuous-countercurrent, multicolumn chromatography. *Bioprocess Int.* 2009, *7*, S18–S23.

[19] Schulte, M., Strube, J., Preparative enantioseparation by simulated moving bed chromatography. *J. Chromatogr. A* 2001, *906*, 399–416.

[20] Guiochon, G., Preparative liquid chromatography. *J. Chromatogr. A* 2002, *965*, 129–161.

[21] Kaczmarski, K., Mazzotti, M., Storti, G., Morbidelli, M., Modeling fixed-bed adsorption columns through orthogonal collocations on moving finite elements. *Comput. Chem. Eng.* 1997, *21*, 641–660.

[22] Baur, D., Angarita, M., Müller-Späth, T., Morbidelli, M., Optimal model-based design of the twin-column CaptureSMB process improves capacity utilization and productivity in protein A affinity capture. *Biotechnol. J.* 2016, *11*, 135–145.

[23] Warikoo, V., Godawat, R., Brower, K., Jain, S. et al., Integrated continuous production of recombinant therapeutic proteins. *Biotechnol. Bioeng.* 2012, *109*, 3018–3029.

[24] Godawat, R., Brower, K., Jain, S., Konstantinov, K. et al., Periodic counter-current chromatography – design and operational considerations for integrated and continuous purification of proteins. *Biotechnol. J.* 2012, *7*, 1496–1508.

[25] Ljunglöf, A., Hjorth, R., Confocal microscopy as a tool for studying protein adsorption to chromatographic matrices. *J. Chromatogr. A* 1996, *743*, 75–83.

[26] Hubbuch, J., Linden, T., Knieps, E., Ljunglöf, A. et al., Mechanism and kinetics of protein transport in chromatographic media studied by confocal laser scanning microscopy: Part I. The interplay of sorbent structure and fluid phase conditions. *J. Chromatogr. A* 2003, *1021*, 93–104.

[27] Linden, T., Ljunglöf, A., Hagel, L., Kula, M.-R., Thömmes, J., Visualizing patterns of protein uptake to porous media using confocal scanning laser microscopy. *Sep. Sci. Technol.* 2002, *37*, 1–32.

[28] Dziennik, S. R., Belcher, E. B., Barker, G. A., Lenhoff, A. M., Effects of ionic strength on lysozyme uptake rates in cation exchangers. I: Uptake in SP Sepharose FF. *Biotechnol. Bioeng.* 2005, *91*, 139–153.

[29] Weaver, L. E., Carta, G., Protein Adsorption on Cation Exchangers: Comparison of Macroporous and Gel-Composite Media. *Biotechnol. Progr.* 1996, *12*, 342–355.

[30] Nativ, M., Goldstein, S., Schmuckler, G., Kinetics of ion-exchange processes accompanied by chemical reactions. *J. Inorg. Nucl. Chem.* 1975, *37*, 1951–1956.

[31] Steinebach, F., Angarita, M., Karst, D. J., Müller-Späth, Th., Morbidelli, M.: Model based adaptive control of a continuous capture process for monoclonal antibodies production. *J. Chrom. A*. 2016, doi:10.1016/j.chroma.2016.03.014.

[32] Kukkonen, S., Lampinen, J., GDE3, the third evolution step of generalized differential evolution. *Evolutionary Computation, 2005. The 2005 IEEE Congress on* 2005, *1*, pp. 443–450.